Journal of Low Temperature Physics, Vol. 43, Nos. 3/4, 1981

Tunneling Spectroscopy on the Superconducting Chevrel-Phase Compounds $Cu_{1.8}Mo_6S_8$ and $PbMo_6S_8$

U. Poppe

Institut für Festkörperforschung, Kernforschungsanlage Jülich, Jülich, West Germany

and H. Wühl

Kernforschungszentrum Karlsruhe, Institut für Technische Physik, und Universität Karlsruhe, Karlsruhe, West Germany

(Received November 26, 1980)

The Chevrel-phase compounds $PbMo_6S_8$ and $Cu_{1.8}Mo_6S_8$ have been investigated by tunneling spectroscopy. These superconductors show a very strong electron–phonon interaction expressed by $4 \leq 2\Delta_0/kT_c \leq 5$. Structures in the tunneling density of states have been observed at most energies where the phonon spectra show maxima. The coupling of high-energy modes of the Mo_6S_8 units and of modes associated with displacements of the Pb (Cu) atoms are discussed.

1. INTRODUCTION

The ternary molybdenum chalcogenides $M_xMo_6S_8$ and $M_xMo_6Se_8$ have attracted great interest because of unusual superconducting properties, especially their behavior in high magnetic fields.[1–3]

Efforts have been made to understand the electronic system by band-structure calculations[4–7] and the lattice dynamics in particular by inealstic neutron scattering experiments.[8–10] However, not much is known about the electron–phonon interaction in these Chevrel-phase compounds. There has been some qualitative information on the coupling strength from measurements of the specific heat[8,11,12] as well as NMR and EPR.[13,14] Experimental information on the coupling of individual phonon modes to the electron system have only been given by measurements of the isotopic effect.[15–18]

In this work we present the results of tunneling experiments on $Cu_{1.8}Mo_6S_8$ and $PbMo_6S_8$.[19,20] The measurements of the energy gap Δ_0 show that both substances have very strong electron–phonon interaction.

0022-2291/81/0500-0371$03.00/0

Furthermore, we were able to observe phonon-induced structures in the single-particle density of states obtained from measurements of the first and second derivatives of the current–voltage characteristic of tunnel junctions.

Using a molecular crystal model in which the lattice vibrations are grouped into high-frequency internal modes of the Mo_6S_8 building blocks and low-frequency external modes of the Mo_6S_8 blocks and the M atoms, suggestions have been made that the low-lying optical modes of the metal ions[21] (Pb and Cu in our case) or the torsional modes of the quasirigid Mo_6S_8 units[8,9,22] play a special role for the electron–phonon coupling in Chevrel-phase compounds. The importance of internal modes of the Mo_6 octahedra has been emphasized by recent band-structure calculations of Andersen *et al.*[5]

Lattice dynamical calculations for $PbMo_6S_8$ have shown that there exists appreciable internal–external mode mixing.[23] Thus, for example, the torsional motion of the Mo_6 octahedra is strongly hybridized with an internal breathing mode of the Mo_6 octahedra. We find in our tunneling experiments that most of the phonon modes contribute to the electron–phonon interaction. Modes which are assumed to be dominated by displacements of the M atoms Pb or Cu, however, seem to be of less importance, whereas high-frequency modes seem to couple particularly strongly.

As in other high-T_c superconductors, such as A-15 compounds[24,25] or the transition metal carbides and nitrides,[26] many difficulties have to be overcome in preparing good tunnel junctions of the ternary molybdenum chalcogenides. Since the Fermi velocity is quite small in transition metal compounds, the sampling depths of the tunneling electrons, especially at high energies where the mean free path is limited by phonon emission, is rather short.[27] This means that for good tunneling junctions, it is essential to have stoichiometric, undisturbed, and clean material just below the tunneling barrier. As it is quite difficult to get ternary substances with the required properties by evaporation or sputtering techniques, we started from bulk material in preparing our tunnel junctions.

Two methods were used for the fabrication of the junctions: In the case of $Cu_{1.8}Mo_6S_8$ we made point contacts with oxidized aluminum or GaAs tips which were pressed onto the Chevrel-phase surface very carefully by a piezoelectric drive. The apparatus, which is described elsewhere,[19] was a combination of a mechanical screw drive for coarse adjustment of the point contact and a piezoelectric bending element for fine adjustment. Difficulties arose from the sensitivity to unavoidable mechanical vibrations and, in the case of oxidized Al tips, from short-circuits in the insulating oxide barrier.

More stable junctions were obtained by depositing artificial tunneling barriers onto single crystals of $PbMo_6S_8$ and completing the junction with an Al film. Silicon or oxidized Al films served as barrier.

2. SAMPLE PREPARATION

The $Cu_{1.8}Mo_6S_8$ sample was prepared by reacting the powdered elements at 1200°C for 30 h in a molybdenum crucible closed by electron-beam welding. After the reaction the compound was rendered molten by heating the crucible up to about 1850°C for a few minutes before switching off the oven. The top of the solidified ingot was formed by several single-crystalline areas covered by a thin molybdenum layer. This layer could easily be peeled off, unveiling an extremely clean and smooth surface of the Chevrel phase. On this surface the tunneling point contact was formed. The inductively measured T_c of the $Cu_{1.8}Mo_6S_8$ sample was 10.2 K with a transition width of about 1 K.

The aluminum tips for the point contact were made from 99.999% aluminum wire, which was electropolished in a one mole $Mg(ClO_4)_2$ methanol solution at a current density of about 1 mA/mm.[2] The tips were rinsed in a hot distilled water and purified ethanol. The shiny tips had a radius of about 0.2 mm and were oxidized in air for about 15 min. For the GaAs tips we used Zn-doped material with a density of 2.8×10^{19} carrier/cm^3. These tips were etched in $H_2SO_4+H_2O_2+H_2O$ (3:1:1) and washed in ethanol. Ohmic contact to the tips was made with a eutectic Ga–Al alloy.

In the case of $PbMo_6S_8$ we used small single-crystalline cubes with a length of 0.3–0.4 mm, as shown in Fig. 1. The crystals were prepared by a solid-state diffusion process. We started with coarse-grained $PbMo_6S_8$ powder obtained by heating the compounds to 1300°C in quartz ampules and annealing the reacted powder for about four days at this temperature. Crystals with dimensions of about 30 μm were selected from this material and placed into $PbMo_6S_8$ powder with a grain size of less than 5 μm. After annealing at 1300°C for 15 h, the powder surrounding the grown crystals was replaced by new fine material and the crystals were heated again. A repetition of this process for about six times lead to single crystals with shiny and smooth (100) surfaces which were suitable for the deposition of the artificial barrier. In some cases we used freshly cleaved crystals, leading to the same results. The composition of the starting materials differed by an excess of about 10% Mo from the stoichiometric formula $PbMo_6S_8$ to achieve good crystal growing conditions. The crystals had a T_c of 11.3–12 K and a transition width of about 0.3 K.

The $PbMo_6S_8$ tunnel junctions were prepared as follows: The crystals mounted on a sample holder were contacted with silver paint and the tunneling area was defined by masking the surface with GE varnish. Then the crystals were cooled to 77 K in a vacuum of about 2×10^{-9} Torr and a layer of Al with a thickness of 10–40 Å was evaporated at a partial pressure

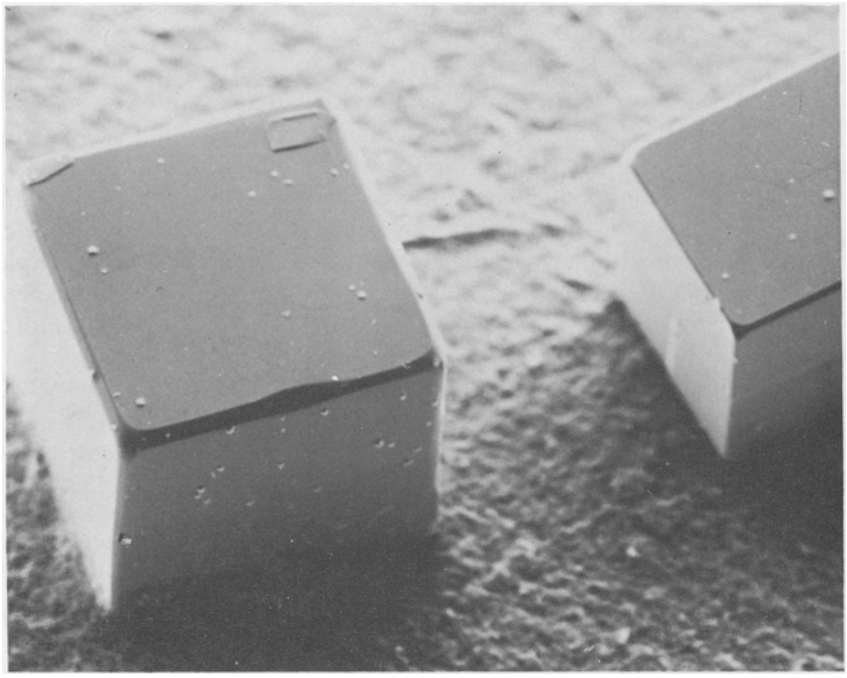

Fig. 1. SEM picture of $PbMo_6S_8$ single crystals.

of about 3×10^{-6} Torr O_2. The deposition rate was 0.7–1.5 Å/sec. The resulting granular AlO_x film was then oxidized for 2 h in pure oxygen at a pressure of 400 Torr and a temperature of 50°C. Then 1000 Å Al was deposited as a counterelectrode at a pressure of about 2×10^{-7} Torr. In a few cases Pb was used instead of Al. Experiments with other kinds of artificial barriers, such as Formvar,[28] wax,[29] or carbon,[25,30] did not lead to observable tunneling currents. Only in the case of Si were we able to measure an energy gap. The best results were achieved with the $PbMo_6S_8/AlO_x/Al$ junctions described above.

For the measurements of the current–voltage characteristics of tunneling junctions and their derivatives dI/dV and d^2I/dV^2 conventional methods have been used.[31,32] For the arrangement normal metal/insulator/superconductor, the first derivative at $T \to 0$ is proportional to the single-particle density of states. Besides the superconducting energy gap Δ_0, phonon-induced structures can be observed at energies exceeding Δ_0. Maxima in $\alpha^2F(\omega)$, which is the phonon spectrum times an average electron–phonon coupling function, produce a decrease in dI/dV. The second

derivative directly reflects the shape of $\alpha^2F(\omega)$. The quality of our junctions was not good enough to give results suitable for a numerical evaluation of $\alpha^2F(\omega)$.

3. RESULTS

First derivatives dI/dV typical for $Cu_{1.8}Mo_6S_8$ point contacts and $PbMo_6S_8/AlO_x/Al$ sandwich junctions are shown in Figs. 2 and 3. The smearing of the gap structure might be due to imperfect barriers and surfaces besides the influence of the finite measuring temperature. A further reason for the smearing in the case of point contacts is an inhomogeneous pressure distribution at the contact area in connection with a strong pressure dependence of T_c in $Cu_{1.8}Mo_6S_8$.[33] The transition temperatures deduced from the vanishing of the energy gap were pressure-enhanced from 10.2 K to 12.5 K. From the plastic deformation of the Al tip we estimate a maximum pressure of 4 kbar at the contact area. The agreement of the observed T_c with pressure with data in the literature proves that the point contact does not notably damage the complicated lattice structure and thus the superconducting properties of the Chevrel phase. Ratios of the junction impedances R_s/R_n, R_s and R_n being measured at zero bias in the superconducting and normal states, respectively, up to 30 were observed for the point contacts. $PbMo_6S_8$ sandwich junctions with the artificial Al oxide barrier usually had ratios of 2–5. In two cases, however, R_s/R_n exceeded 10^4.

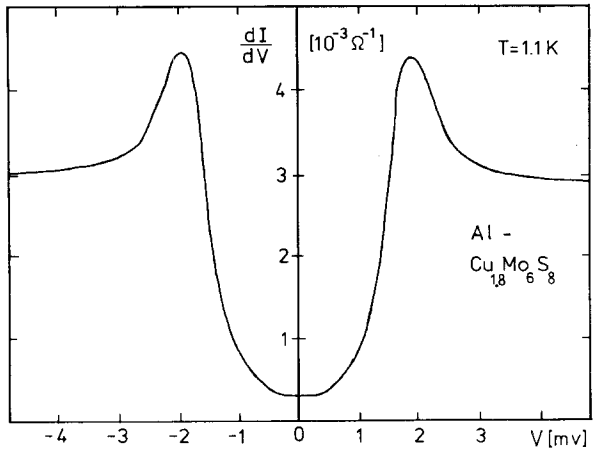

Fig. 2. Differential conductance dI/dV vs. voltage of a $Cu_{1.8}Mo_6S_8$–Al point contact.

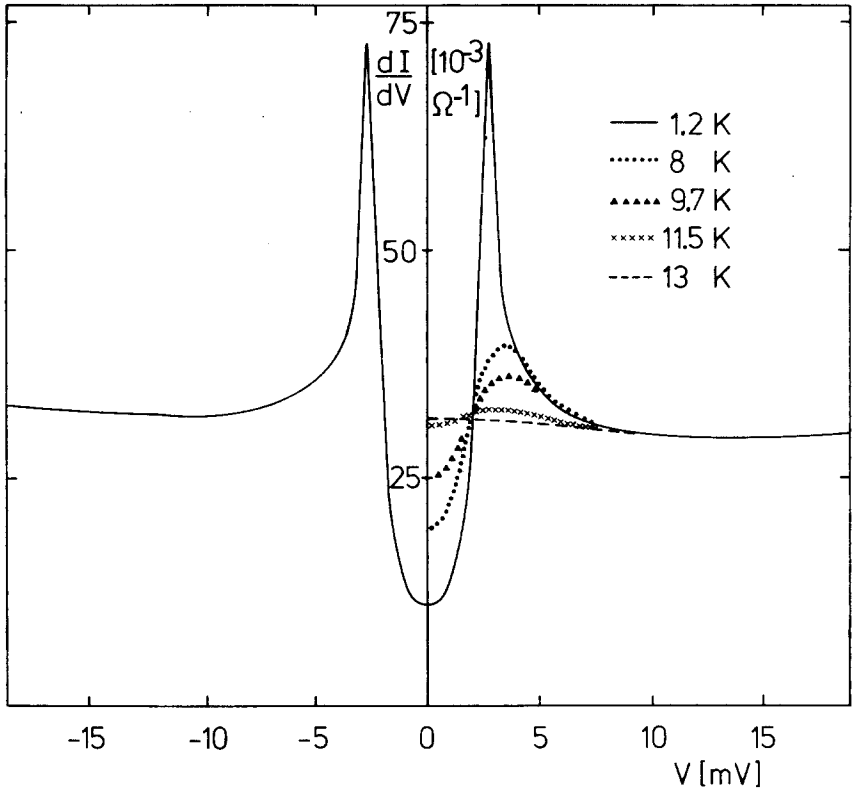

Fig. 3. Differential conductance dI/dV of a $PbMo_6S_8/AlO_x$(12 Å)/Al sandwich junction at various temperatures.

For the evaluation of the energy gap Δ_0, the temperature smearing at $T = 1.2$ K has been taken into account by reducing the energy of the maximum in dI/dV by 7%.[34] This procedure seemed to us more appropriate than other methods,[35] as the gap smearing of our junctions may not be dominated by thermal effects. Thus, energy gaps between 1.8 and 2.3 meV are obtained for $Cu_{1.8}Mo_6S_8$ with different T_c values using the point contact method. The ratios of $2\Delta_0/kT_c$ for which the local T_c was measured in each experiment range from 3.9 to 4.2. For $PbMo_6S_8$, $\Delta_0 = 2.4$ meV and $2\Delta_0/kT_c = 4.8$ are typical values. In some cases values up to 5.5 are observed. These values, significantly exceeding the BCS value of 3.5, indicate extremely strong electron–phonon coupling in these materials. When the energy gap is taken as a lower limit at $dI/dV = R_n^{-1}$,[35] values up to 4.2 are obtained for $2\Delta_0/kT_c$ of $PbMo_6S_8$.

Phonon-induced structures in dI/dV and d^2I/dV^2 were observed for most of the junctions. But instabilities in the tunneling barriers gave rise to excessive noise, especially at high energies, and prevented the analysis of the data in many cases. The more stable junctions were tested for structures due to nontunneling currents through weak spots in the barrier by measuring at different temperatures, since the position and shape of such structures are strongly temperature dependent, in contrast to structures correlated with

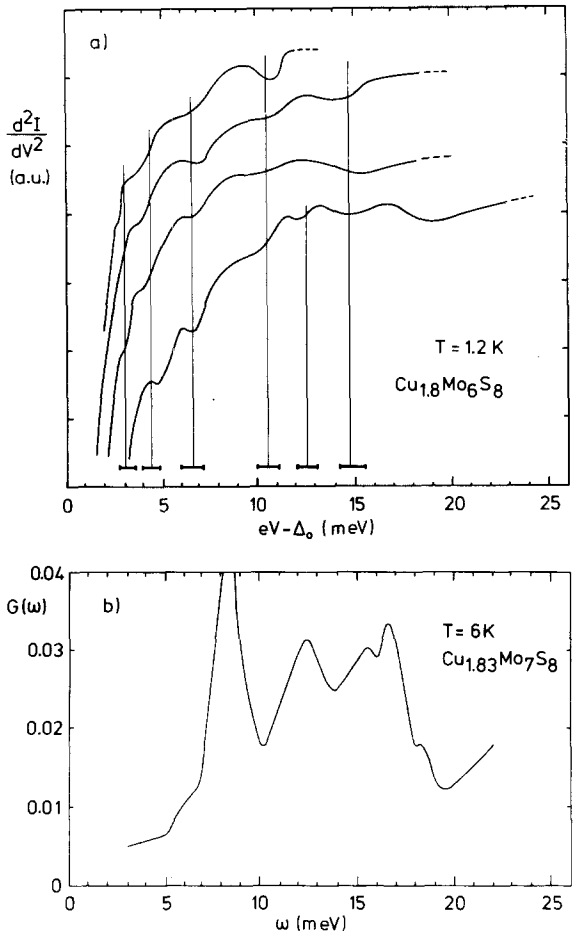

Fig. 4. (a). d^2I/dV^2 vs. voltage measured from the gap edge for four $Cu_{1.8}Mo_6S_8$–Al point contact junctions. The bars show the positions of the minima obtained from about 20 junctions. (b) Phonon density of states $G(\omega)$ from inelastic neutron scattering measured by Schweiss *et al.*[10]

the Eliashberg functions $\alpha^2F(\omega)$. At $T > T_c$ the tunneling characteristics were completely smooth. At energies $\omega \leq 20$ meV, structures due to peaks in $\alpha^2F(\omega)$ could be reproduced for more than 30 junctions, whereas at $\omega > 20$ meV phonon-induced structures could be only observed in a few junctions of the type $PbMo_6S_8/AlO_x/Al$.

The best information on $\alpha^2F(\omega)$ at $\omega < 20$ meV was obtained for $Cu_{1.8}Mo_6S_8$ using point contacts. In Fig. 4a traces of d^2I/dV^2 from different samples demonstrate the reproducibility. The magnitude of the dips in d^2I/dV^2 varies, depending on the quality of the junctions. The influence of the contact pressure on phonon frequencies is expected to be of minor importance. The bars mark the variation of the energetic position of the minima obtained from all our measurements. The low-energy part of the generalized phonon density of states $G(\omega)$ obtained by neutron scattering experiments[10] at 5 K[10] are shown for comparison in Fig. 4b.

At most energies where characteristic phonons appear in $G(\omega)$, minima in d^2I/dV^2 are observed. Qualitative agreement between both results exists at energies of about 4.5, 6.5, 12.5, and 15 meV. The phonon peak at 12.5 meV, reflected as a well-pronounced minimum in only one of the second derivatives shown in Fig. 4a, has been observed in four other (not shown) experiments. The existence of a phonon peak at 3 meV could not be confirmed, since elastic neutron scattering dominates at such low energies. Disagreement exists at 8.5 and 10.5 meV. The Einstein-like phonon peak at 8.5 meV shows a very weak structure observed only occasionally in d^2I/dV^2. On the other hand, the structure in d^2I/dV^2 at 10.5 meV has no counterpart in $G(\omega)$.

Measurements at high energies could be considerably improved by changing from the point contact junction to $PbMo_6S_8/AlO_x/Al$ sandwich junctions. Here only dI/dV has been measured. The differential conductance of a junction measured in the superconducting and normal states is shown in Fig. 5. The relatively strong suppression of the conductance in the superconducting state below that of the normal state, especially from 6 to 28 meV, implies the coupling to a broad band of phonons which is not much structured. Peaks in $\alpha^2F(\omega)$ expected from dI/dV are marked by arrows. Maxima in $G(\omega)$ are indicated on the abscissa. The agreement in the energy positions is fairly good. Similar results were obtained on three additional junctions. The magnitude of the steps at high energies amounts to about 1% of the junction resistance. Apparently, our junctions are of sufficiently high quality that, in spite of the small sampling depth, phonon-induced structures representing the bulk material could be resolved at energies up to 50 meV.

Since the height of a step in dI/dV due to a peak in $\alpha^2F(\omega)$ is weighted with ω^{-2}, the pronounced steps at $\omega > 20$ meV indicate a very strong coupling at energies where the internal modes of the Mo_6S_8 unit dominate.

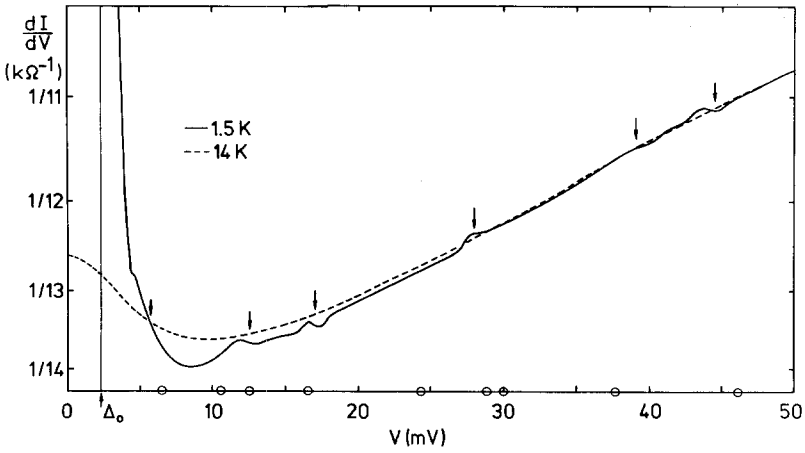

Fig. 5. Differential conductance dI/dV of a $PbMo_6S_8/AlO_x/Al$ tunneling diode versus voltage measured at 1.5 and 14 K. The arrows indicate peaks in $\alpha^2F(\omega)$. The energies of characteristic peaks in the phonon density of states (0) as determined from inelastic neutron scattering in Ref. 10 are indicated from the gap edge Δ_0.

In the energy range of vibrations attributed to the displacement of the Pb atom ($\omega \approx 4$ meV) the peak in $\alpha^2F(\omega)$ lies 0.5–1 meV below that of $G(\omega)$.

4. DISCUSSION

The comparison of tunneling data with the generalized phonon spectra of Chevrel-phase compounds has shown that both low-frequency and high-frequency modes contribute to the electron–phonon interaction. The results indicate that high-frequency internal modes are of special importance. At low energies discrepancies between $G(\omega)$ and the tunneling data are evident.

$Cu_{1.8}Mo_6S_8$ undergoes a structural phase transformation at 269 K, which has a substantial effect on the low-energy part of $G(\omega)$.[10] In the low-temperature modification the Cu atoms condense into pairs, causing a small triclinic distortion of the lattice.[36] This distortion is likely to cause a splitting into different optical branches associated with Cu atom displacements. The pronounced Einstein-like peak which appears in connection with the phase transformation in $G(\omega)$ at 8.5 meV can be attributed to one of these optical modes. The absence of comparably strong structure in d^2I/dV^2 at 8.5 meV indicates weak coupling to this special mode. The slight shift in energy observed for $PbMo_6S_8$ around 4 meV may be due to a similar reason. The results on $Cu_{1.8}Mo_6S_8$ imply that there is a special mode at 10.5 meV which is not distinguished in $G(\omega)$ but contributes to $\alpha^2F(\omega)$. The

amount of hybridization of low-frequency modes with internal modes seems to be decisive for the coupling to the electron system.

For a more quantitative analysis of the discrepancies between $G(\omega)$ and the tunneling results, the different constitution and the very different stoichiometry* of the samples used in the experiments must possibly also be considered.

The calculation of $\alpha^2F(\omega)$, and thus of the electron–phonon coupling constant λ, has not been possible, because of instabilities in the junctions. A measure of the integral coupling strength is the ratio $2\Delta_0/kT_c$. Values approaching 5.0 in the case of $PbMo_6S_8$ are among the highest reported in literature. Values of about 5 have also been extracted from EPR measurements on Gd in $PbMo_6S_8$ and $SnMo_6S_8$.[14] On the assumption that the superconducting behavior is basically the same for all Chevrel-phase compounds, we include in our discussion a binary system. The analysis of specific heat data on carefully prepared, single-phase Mo_6Se_8 yielded $2\Delta_0/kT_c = 4.2$.[12,37] The jump in the electron specific heat at T_c, $(C_s - C_n)/C_n = 2.25$, which is 1.6 times the BCS value (and considerable phonon softening on cooling, as observed in several Chevrel-phase compounds[8–10]) emphasizes strong electron–phonon coupling. It is remarkable that this binary low-T_c compound ($T_c = 6.3$ K) already shows strong coupling behavior.

Band-structure calculations[5] have shown that superconductivity is primarily associated with the d electrons of the Mo_6 octahedra. Since it is mainly the charge fluctuations that correspond to motions of Mo atoms of the immediate neighborhood that lead to a pairing of d electrons, electron–phonon interaction should be primarily determined by the coupling of internal modes of the Mo_6 octahedra to the Mo d electrons.[5,16] Therefore displacements of the M atoms as well as of the Mo_6S_8 units may contribute to superconductivity only to the extent that these modes are hybridized with internal modes of the Mo_6 octahedra. Since the energies where hybridization takes place in general do not coincide with those of Brillouin-zone boundary modes, phonons with a relatively small density of states may experience a high electron–phonon coupling, leading to an enhanced peak in $\alpha^2F(\omega)$. These effects of hybridization seem to be observed in our tunneling experiment.

So the M atoms influence superconductivity mainly in an indirect way by charge transfer to the $Mo_6S_8(Se_8)$ units, which reduces the distortion of the Mo_6 octahedra and alters the electron density of states at the Fermi level.[39]

* The starting compositions for the samples used in our work are $Pb_{1.07}Mo_{6.75}S_8$ and $Cu_{1.8}Mo_6S_8$, while for the neutron scattering experiments in Ref. 10 the compositions $Pb_{1.02}Mo_{5.7}S_8$ and $Cu_{1.83}Mo_7S_8$ were used.

Information on the interaction between electrons and phonons had already been obtained by the analysis of the isotope effect in Mo_6Se_8. Culetto and Pobell[15] have shown that a dominant coupling of a soft torsional mode must be excluded. Further, it was concluded that the internal modes are at least as important for superconductivity in Mo_6Se_8 as the external modes. The analysis of the isotope effect in ternary $SnMo_6S_8$ is more difficult because of the large dependence of T_c on stoichiometry. Results are incongruous and a zero as well as an inverse isotope effect has been deduced from the data.[18,40,41,42]

In conclusion, the tunneling experiments on $Cu_{1.8}Mo_6S_8$ and $PbMo_6S_8$ show that these materials have a very strong electron–phonon coupling. Both high-frequency modes and low-frequency modes couple to the electrons. The results emphasize the importance of the high-frequency modes for superconductivity. The contribution of low-frequency modes seems to depend on the amount of hybridization with internal modes of the Mo_6 unit.

ACKNOWLEDGMENTS

We would like to thank Prof. F. Pobell, Dr. F. J. Culetto, Prof. D. Rainer, Dr. B. P. Schweiss, and Dr. B. Renker for many helpful discussions. The support of the crystal laboratory of the Institut f. Festkörperforschung, KFA Jülich, is gratefully acknowledged.

REFERENCES

1. Ø. Fischer, R. Odermatt, G. Bongi, H. Jones, R. Chevrel, and M. Sergent, *Phys. Rev. Lett.* **45A**,, 87 (1973).
2. S. Foner, E. J. McNiff, and E. J. Alexander, *Phys. Lett. A* **49**, 269 (1976).
3. Ø. Fischer, *Appl. Phys.* **16**, 1 (1978).
4. L. F. Mattheis and C. Y. Fong, *Phys. Rev. B* **15**, 1760 (1977).
5. O. K. Andersen, W. Klose, and H. Nohl, *Phys. Rev. B* **17**, 1209 (1978).
6. D. W. Bullet, *Phys. Rev. Lett.* **39**, 664 (1977).
7. T. Jarlborg and A. J. Freemann, *Phys. Rev. Lett.* **44**, 178 (1980).
8. S. D. Bader, G. S. Knapp, S. K. Sinha, B. P. Schweiss, and B. Renker, *Phys. Rev. Lett.* **37**, 334 (1976).
9. B. P. Schweiss, B. Renker, E. Schneider, and W. Reichardt, in *Superconductivity in d- and f-Band Metals*, D. H. Douglass, ed. (Plenum, New York, 1976), p. 189.
10. B. P. Schweiss, B. Renker, and R. Flükiger, in *Proceedings of the Internat. Conf. on Ternary Superconductors* (Lake Geneva, 1980).
11. F. Y. Fradin, G. S. Knapp, S. D. Bader, G. Cinader, and C. W. Kimball, in *Superconductivity in d- and f-Band Metals*, D. H. Douglass, ed. (Plenum, New York, 1976), p. 297.
12. K. P. Nerz, Thesis, Universität Bochum (1979), Bericht der Kernforschungsanlage Jülich, Jül-Spez-30.
13. N. Sano, T. Taniguchi, and K. Asayama, *Solid State Comm.* **33**, 319 (1980).
14. R. Odermatt, M. Hardiman, and I. von Meijle, *Solid State Comm.* **32**, 1227 (1979).
15. F. J. Culetto and F. Pobell, *Phys. Rev. Lett.* **40**, 1104 (1978).
16. F. J. Culetto and D. Rainer, *Phys. Rev. B* **19**, 2540 (1979).

17. F. J. Culetto and D. Rainer, Bericht der Kernforschungsanlage Jülich, Jül-1504 (1978).
18. N. E. Alekseevskij and V. I. Ninankovaoskij, *JETP Lett.* **31**, 58 (1980).
19. U. Poppe, Thesis, Universität Köln (1979), Bericht der Kernforschungsanlage Jülich, Jül-1635 (1980).
20. U. Poppe and H. Wühl, *J. Phys.* (*Paris*) **39**, C6-361 (1978).
21. C. W. Kimball, L. Weber, G. van Landuyt, F. Y. Fradin, B. D. Dunlap, and G. K. Shenoy, *Phys. Rev. Lett.* **36**, 412 (1976).
22. S. D. Bader, S. K. Sinha, and R. N. Shelton, in *Superconductivity in d- and f-Band Metals*, D. H. Douglass, ed. (Plenum, New York, 1976), p. 209.
23. S. D. Bader and S. K. Sinha, *Phys. Rev. B* **18**, 3082 (1978).
24. L. Y. Chen, *Phys. Lett.* **29**, 1082 (1972).
25. D. F. Moore, J. M. Rowell, and M. R. Beasley, *Solid State Comm.* **20**, 305 (1976).
26. J. Geerk, W. Gläser, F. Gompf, W. Reichardt, and E. Schneider, in *Proc. 14th Conference on Low Temperature Physics*, M. Krusius and M. Vuorio, eds. (Helsinki, 1975), Vol. 2, p. 411.
27. E. L. Wolf, *Rep. Prog. Phys.* **41**, 1439 (1978).
28. G. Burrafato, G. Faraci, G. Giagunta, and N. A. Mancini, *J. Phys. C* **5**, 2179 (1972).
29. G. Beuermann, *Z. Physik B* **28**, 201, 207 (1977).
30. M. MacVicar, *J. Appl. Phys.* **41**, 1965 (1970).
31. J. G. Adler and J. E. Jackson, *Rev. Sci. Instrum.* **37**, 1049 (1966).
32. T. L. Paoli and J. F. Svacek, *Rev. Sci. Instrum.* **47**, 1016 (1976).
33. R. N. Shelton, in *Superconductivity in d- and f-Band Metals*, E. Burstein and S. Lundquist, eds. (Plenum, New York, 1969), p. 233.
34. S. Bermon, Technical Report No. 1, NSF-GP 1100, University of Illinois (1964).
35. W. L. McMillan and J. M. Rowell, in *Superconductivity*, R. D. Parks, ed. (Marcel Dekker, New York, 1969), p. 561.
36. K. Ivon, R. Balif, and R. Flükiger, *Acta Cryst. B* **35**, 2859 (1979).
37. K. P. Nerz, U. Poppe, F. Pobell, M. Weger, and H. Wühl, in *Proceedings of the 3rd Conf. on Superconductivity in d- and f-Band Metals* (La Jolla, June 1979).
38. K. Yvon and A. Paoli, *Solid State Comm.* **24**, 41 (1977).
39. K. Yvon, in *Current Topics in Material Science*, E. Kaldis, ed. (North-Holland, Amsterdam, 1978), Vol. 3, p. 53.
40. F. J. Culetto, Thesis, Techn. Universität Wien (1979), Bericht der Kernforschungsanlage Jülich, Jül-1587 (1979).
41. F. Pobell, in *Proceedings of the Internat. Conf. on Ternary Superconductors* (Lake Geneva, 1980).